View metadata, citation and similar papers at core.ac.uk

brought to you by CORE

provided by NASA Technical Reports Server

PREDICTION OF THE DRAG COEFFICIENT OF A 20-DEGREE CONICAL RIBBON PARACHUTE

By

Jajpat R. Utreja

September 1975

Backup Document for AIAA Synoptic Scheduled
for Publication in the Journal of Spacecraft and Rockets, January 1977

Aeromechanics Branch
Northrop Services Inc.
6025 Technology Drive
P. O. Box 1484
Huntsville, Alabama 35807

TN-230-1523

PREDICTION OF THE DRAG COEFFICIENT OF A 20-DEGREE CONICAL RIBBON PARACHUTE

September 1975

by

Lajpat R. Utreja

PREPARED FOR:

NATIONAL AERONAUTICS AND SPACE ADMINISTRATION
GEORGE C. MARSHALL SPACE FLIGHT CENTER
SCIENCE AND ENGINEERING DIRECTORATE

Under Contract NAS8-21810

REVIEWED AND APPROVED BY:

W. W. Boyle

W. W. Boyle, Manager
Aero-Mechanics Branch

FOREWORD

This technical note presents the result of work performed by Northrop Services, Inc., Huntsville, Alabama, under Contract NAS8-21810 to the Systems Dynamics Laboratory of the Marshall Space Flight Center. This work was conducted in partial response to the requirements of Appendix B, Schedule Order B02Z (B-64). Technical coordination was provided by Mr. David L. Bacchus of the Aerodynamics Analysis Branch, ED32.

TABLE OF CONTENTS

LIST OF ILLUSTRATIONS

LIST OF TABLES

Abstract

An empirical formula for the steady-state drag coefficient of a 20-degree conical ribbon parachute is developed. The derived expression takes into account the effect of suspension line length and geometric porosity within the limits of practical design. Also included are factors which provide drag reduction due to skirt reefing and the wake behind a primary body. The calculated values are in agreement with the available experimental results.

Nomenclature

C_D	Drag coefficient
C_{D_1}	Drag coefficient of a parachute with $L_s = D_o$ and $\lambda_g = 0\%$
C_{D_∞}	Free stream drag coefficient
D	Drag force
D_B	Forebody diameter
D_o	Parachute nominal diameter (diameter of a circle with area equal to S_o)
D_p	Parachute projected diameter
f(x,y)	Function of x and y
K	Forebody interference factor
L_R	Length of reefing line
L_s	Length of suspension line
q	Dynamic pressure
S_o	Parachute reference area
x	Trailing distance from forebody to canopy skirt
λ_g	Geometric porosity

I. Introduction

Numerous experiments have been conducted on different kinds of parachutes to investigate their performance characteristics. To date, it has not been generally possible to express the drag coefficient of a parachute in terms of its design parameters. One reason is that when a parachute was tested, it was generally designed for a particular mission and no attempt was made to study the variation of design parameters. Moreover, a general expression for the drag coefficient of a parachute was difficult to obtain because tests usually used parachutes with different design characteristics, for example, canopy loading, porosity, and flexibility, etc.

In July 1974, parametric tests were conducted on a 20-degree conical ribbon parachute. This parachute configuration has been selected as the drogue parachute for the Space Shuttle Solid Rocket Booster recovery system. Based on the numerous wind tunnel and drop test data available on the 20-degree conical ribbon parachute, it is desirable to develop relationships which will allow the prediction of performance over a range of configuration parameters.

The ribbon parachute consists of a large number of concentrically placed ribbons. These ribbons, known as horizontals, are held at close intervals by one or more verticals. The radials extend from the skirt to the vent and form the bounds of a gore (see Fig. 1). The conical ribbon canopy is similar to the flat circular ribbon canopy, with a few gores removed to give it a conical profile. An important characteristic of ribbon parachutes is their low opening shock and increased stability compared to solid parachutes. Heavy duty ribbon parachutes have been designed in the past for high speed deployment and for recovery of large loads.

Aerodynamic characteristics of a conical ribbon parachute depend upon its design parameters, for example, cone angle, geometric porosity, and suspension line length. These design parameters govern the shape of the inflated canopy and thereby influence parachute performance. An established reference on parachute design is the Air Force Parachute Handbook.[1] A designer often uses the values of the force coefficients given in the parachute handbook for preliminary design analyses. The handbook lists, for the drag coefficient of a conical ribbon parachute, a range of 0.45 to 0.55 with an average value of 0.50. Recent wind tunnel parametric tests of a 20-degree conical ribbon parachute[2] have shown that for a given combination of suspension line length and geometric porosity, the drag coefficient may be in the range specified, but it may also be outside the range. For example, the drag coefficient of a 20-degree conical ribbon parachute with suspension line length ratio of 1.75 and geometric porosity of 16% is estimated to be 0.672 as compared to an average value of 0.5 given in the parachute handbook. It is thus desirable to improve the methods of predicting the drag coefficient to include the effect of design parameters.

The purpose of this report is to present the formulation of a mathematical expression for the steady-state drag coefficient of a 20-degree conical ribbon parachute in subsonic flow. This expression takes into account the effect of the suspension line length, geometric porosity, reefing line lentgh, and the wake effects behind a primary body. The empirical relationship derived is for a particular porosity distribution used in the SRB drogue parachute models as illustrated in Figure 1. This porosity distribution is characterized by equally spaced horizontal ribbons. Variation in geometric porosity is achieved by varying the gap size, keeping the apex vent size constant. In contrast to this design, variable porosity conical ribbon parachutes have been designed for specific applications.

II. Mathematical Model

Drag of a body in motion is defined as the component of aerodynamic forces in the direction of the relative wind. Steady-state refers to a state of uniform motion with no acceleration. In the case of a parachute canopy, the drag force is defined as,

$$D = C_D S_o q \qquad (1)$$

where

C_D is the drag coefficient.

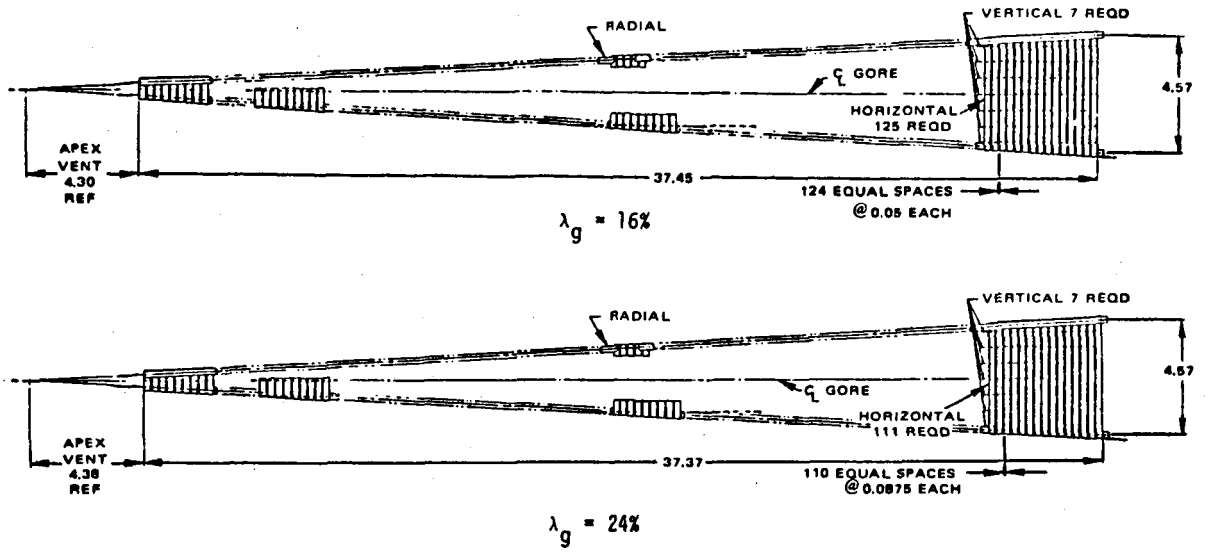

Fig. 1. Detail gore assemblies of the SRB drogue parachute models

S_o is the nominal area of the conical ribbon canopy which is equivalent to the total surface area that produces drag including vent area and the area of openings not covered by ribbons.

q is the dynamic pressure.

In the case of a parachute being tested in the wind tunnel, steady-state refers to a state when the canopy, after having deployed, has completed the filling process and has attained a fixed shape based on its geometry and design characteristics.

Equation (1) provides drag force along the longitudinal axis of the parachute in steady-state. The drag coefficient, C_D, for a given parachute and flight condition is expressible in terms of several design parameters. These parameters are canopy geometric porosity, suspension line length, and the reefing line length.

The following restrictions have been made which limit the validity of the empirical relationship as to the size of the parameters and the parachute operating envelope.

1. The data on 20-degree conical ribbon parachutes is available for a limited range of canopy geometric porosity, thus the expression for C_D is considered in agreement for the range, $10\% < \lambda_g < 30\%$ available for comparison. This range is believed to be reasonable from the standpoint of practicality. The lower limit takes into account the complexity of fabrication which increases with a reduction in geometric porosity. The upper limit establishes a maximum value for standard parachute design.

2. The shortest suspension line length considered is one nominal diameter. This is justified from the standpoint of canopy performance. Reducing suspension line length below one nominal diameter results in a considerable decrease in the projected diameter and thus, a loss of parachute efficiency as a drag producing surface. Also, traditionally, the length of the lines on most canopies is about one nominal diameter.

3. The aeroelastic effects on the canopy are neglected. This is a reasonable approximation if the dynamic pressure is comparatively small[3]. Elasticity of the cloth changes the way the drag force varies with other design parameters. Thus, in any flight envelope where the dynamic pressure is high so that the induced strains produce canopy shape changes, there will be an aeroelastic effect. However, for the present study we are concerned with low steady-state dynamic pressures and the assumption seems reasonable.

4. The minimum trailing distance considered is one nominal diameter. This follows from assumption (2) in which the minimum suspension line length considered is one nominal diameter.

In the present study the drag coefficient of a solid (zero geometric porosity) 20-degree conical ribbon parachute having a suspension line length equal to its nominal diameter is regarded as a basic drag coefficient. The effect of suspension line lengths greater than one nominal diameter, and geometric porosity is introduced by adding correction factors to the basic drag coefficient. The drag coefficient of a reefed canopy is obtained by multiplying the drag coefficient of a full open canopy by the drag area ratio corresponding to a particular reefing line length.

In the following equation the drag coefficient is expressed as a function of the parachute design parameters.

$$C_D = [C_{D_1} + K_{\lambda_g} \cdot f(\lambda_g) + K_{L_s/D_o} \cdot f(L_s/D_o)]K_R \quad (2)$$

Here,

C_{D_1}: steady state drag coefficient of a 20-degree conical ribbon parachute with $\frac{L_s}{D_o} = 1.0$ and $\lambda_g = 0\%$.

K_{λ_g}: correction factor for the drag coefficient of parachutes with geometric porosity.

$f(\lambda_g)$: a function of geometric porosity.

K_{L_s/D_o}: correction factor for the drag coefficient of parachutes with line length ratio of more than one.

$f(L_s/D_o)$: a function of suspension line length.

K_R: ratio of the reefed drag area to the full open drag area based on the nominal area, that is, $K_R = \frac{(C_D S)_R}{(C_D S)_o}$.

In practical applications the parachute is deployed in the wake of a forebody, to decelerate or aid in the recovery of the forebody. The wake of a forebody affects the drag characteristics of a parachute. Effectively, the wake reduces the efficiency of the drag producing surface. Equation (2) can be modified as follows to account for the presence of a forebody.

$$C_D = [C_{D_1} + K_{\lambda_g} \cdot f(\lambda_g) + K_{L_s/D_o} \cdot f(L_s/D_o)] K_R' \cdot K \qquad (3)$$

where K is the forebody interference factor and K_R' is the modified K_R in the presence of a forebody.

Thus, to predict the drag coefficient of a parachute with known design parameters behind a forebody, we need to know the correction factors K_{λ_g}, K_{L_s/D_o}, K_R', and K. There correction factors can be determined analytically if the dependence of the drag coefficient on the selected design parameters is explicitly known. In the absence of such a relationship these factors must be determined empirically. In the following sections an attempt has been made to evaluate the correction factors based on experimental test results and empirical considerations. Design parameters of various size 20-degree conical ribbon parachutes considered in the evaluation of the mathematical formulation are listed in Table 1.

Table 1. Twenty-degree conical ribbon parachute design and environment data.

Parachute Nominal Diameter (ft)	Geometric Porosity, (%)	Number of Gores	Suspension Line Length (ft)	Deployment Dynamic Pressure (lb/ft^2)
1.5	21.4	24	1.5	1.56-3.12
3.0	10-40	24	3.0-6.0	35-75
6.75	16-24	54	6.75-13	20-50
22.2	23	32	23.75	4350
76.0	16	80	80	127-280
45-in	0	-	45-in	-

III. Correction Factors

Canopy Geometric Porosity

Geometric porosity is a design parameter which influences drag, stability, filling time, and opening shock of a particular canopy. Optimum porosity is generally a trade-off between a higher drag efficiency for low geometric porosity chutes and low opening shocks, and increased chute stability for high geometric porosity chutes.

Solid conical ribbon parachutes[4] with various cone angles have been tested in the past and their drag coefficients are reproduced in Figure 2. Wind tunnel experiments have shown that the steady-state drag coefficient of a 20-degree conical ribbon parachute is strongly influenced by its geometric porosity. Figure 3[5] illustrates the variation of the free stream drag coefficient with geometric porosity. It is evident from the figure that for a given suspension line length the drag coefficient decreases with increasing porosity. Also, for different line lengths the slope of C_D vs λ_g curves in the 16-24 percent range is approximately the same. Using Figures 2 and 3, the drag coefficient of a canopy with $L_s/D_o = 1.0$ can be expressed as,

$$C_D = .874 - 2.29\,\lambda_g + 1.953\,(\lambda_g)^2 \qquad (4)$$

Comparing equation (4) with (2) we get,

$$C_{D_1} = .874 \text{ and} \qquad (5)$$

$K_{\lambda_g} \cdot f(\lambda_g)$ is a quadratic function of λ_g. It can be expressed as,

$$K_{\lambda_g} \cdot f(\lambda_g) = K'\lambda_g + K''(\lambda_g)^2 \qquad (6)$$

where

$$K' = -2.29 \qquad (7)$$

and

$$K'' = 1.953\,. \qquad (8)$$

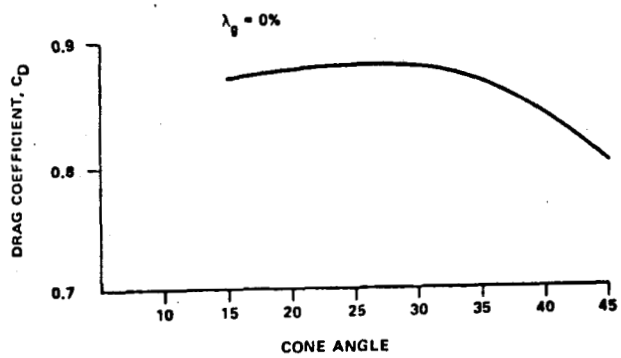

Fig. 2. Effect of cone angle on canopy drag coefficient. (Ref. 4)

Suspension Line Length

The suspension line length is another design parameter which greatly influences the weight

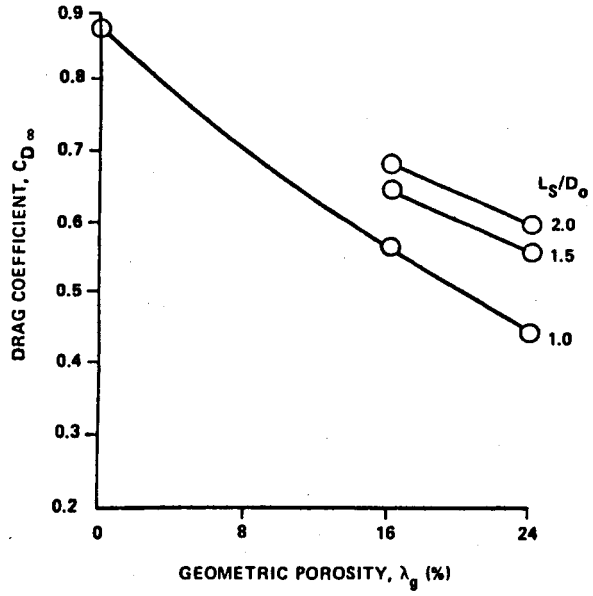

Fig. 3. Effect of geometric porosity on canopy drag coefficient. (Ref. 5)

and the drag of the parachute. An optimum design is usually a trade-off between the drag efficiency (longer suspension lines) and the weight (smaller suspension lines, capable of being stowed in the volume available). Also, increasing the length of the suspension lines is used as a method to improve canopy stability.

Presented on Figure 4 are typical data trends that show the free stream drag coefficient increase with an increase in suspension line length. The two curves, representing geometric porosities of 16 percent and 24 percent, are essentially parallel except at the lower end of suspension line length near $L_S/D_o = 1.0$. This characteristic provides a method of combining the two curves in an average manner; however, K_{L_S/D_o} becomes dependent on both the geometric porosity and the suspension line length, that is:

$$K_{L_s/D_o} = f(\lambda_g, L_s/D_o) \quad . \tag{9}$$

Combining the two curves in Figure 4 in conjunction with equation (4) we get,

$$C_D = 0.874 - 2.29\lambda_g + 1.953(\lambda_g)^2 + (0.055 + 1.145\,\lambda_g)\left(\frac{L_s}{D_o} - 1\right) + (0.012 - 0.775\,\lambda_g)\left(\frac{L_s}{D_o} - 1\right)^2 \quad . \tag{10}$$

Comparing equation (10) with (2) we get,

$$C_{D_1} = 0.874$$

$$K_{\lambda_g} \cdot f(\lambda_g) = -2.29\,\lambda_g + 1.953\,(\lambda_g)^2 \quad .$$

Also K_{L_s/D_o} is a quadratic function of L_s/D_o. It can be expressed as,

$$K_{L_s/D_o} \cdot f\left(\frac{L_s}{D_o}\right) = K_3\left(\frac{L_s}{D_o} - 1\right) + K_4\left(\frac{L_s}{D_o} - 1\right)^2 \tag{11}$$

where K_3 and K_4 are both functions of geometric porosity. From equations (10) and (11),

$$K_3 = 0.055 + 1.145\,\lambda_g \tag{12}$$

and

$$K_4 = 0.012 - 0.775\,\lambda_g \quad . \tag{13}$$

Thus,

$$K_{L_s/D_o} \cdot f\left(\frac{L_s}{D_o}\right) = (0.055 + 1.145\,\lambda_g)\left(\frac{L_s}{D_o} - 1\right) + (0.012 - 0.775\,\lambda_g)\left(\frac{L_s}{D_o} - 1\right)^2 \quad . \tag{14}$$

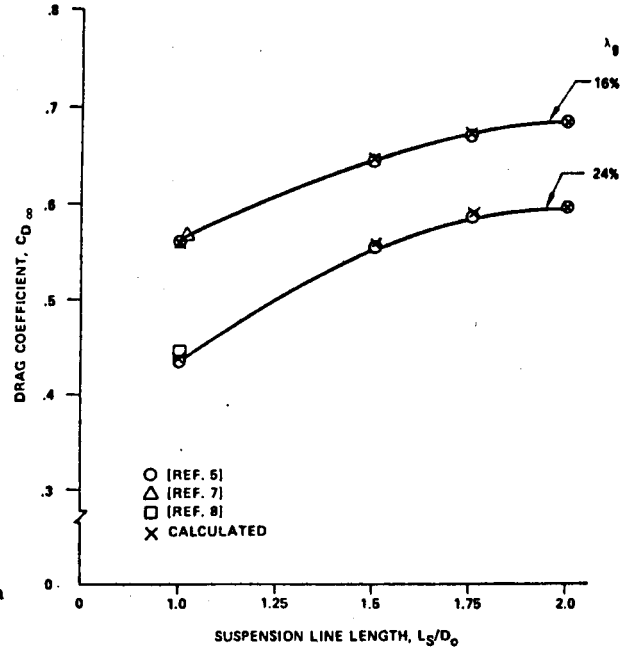

Fig. 4. Effect of suspension line length on drag coefficient.

Reefing Line Length

A parachute is reefed to control its drag area. Thus to obtain drag force at a predetermined value, it is desired to determine the reefing line length. It is conventional to express drag area ratio K_R, that is $(C_DS)_R/(C_DS)_o$ as a function of the reefing ratio (D_r/D_o) as follows,

$$K_R = K_R\left(\frac{D_R}{D_o}\right) \tag{15}$$

Riffle[6] provides a tabulation of the drag coefficients of a 20-degree conical ribbon parachute for different reefing ratios. This parachute had a geometric porosity, λ_g = 21.4% and the line length, L_s/D_o = 1.0. The drag area ratios of this parachute have been plotted against the reefing ratio in Figure 5. The drag area ratios of a 22.2-foot constructed diameter parachute[7] and a 76-foot constructed diameter parachute[8] are presented in Figure 5. These parachutes had an L_s/D_o ratio of approximately one, and geometric porosities of 23% and 16% respectively. Also plotted in this figure is a range of drag area ratios of 20-degrees conical ribbon model parachutes with geometric porosities from 10 to 30 percent[9] and the line length ratio equal to one. It is inferred that even though this range covers a wide range of geometric porosity, in magnitude the variation can be considered as scatter in the data. It seems reasonable to use a mean value of K_R and regard K_R as independent of geometric porosity. Therefore,

$$K_R = 1.735\left(\frac{D_R}{D_o}\right) - .11$$

or

$$K_R = .55\left(\frac{L_R}{D_o}\right) - .11 \qquad (16)$$

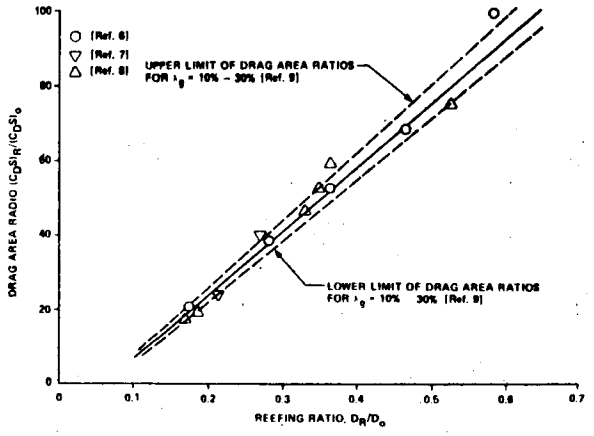

Fig. 5. Effect of reefing ratio on drag coefficient.

It is also evident from Figure 5 that the skirt diameter for a full open parachute is approximately

$$\frac{D_R}{D_o} = 0.64 \qquad (17)$$

or

$$\frac{L_R}{D_o} = 2.011 \qquad (18)$$

A full open canopy corresponds to L_R/D_o = 2.011 and the correction factor K_R = 1.0. Equation (16) can be used to determine the reefing line length providing x percent of the full open drag area.

$$x = .55\left(\frac{L_R}{D_o}\right) - .11$$

or

$$L_R = (x + .11)\, D_o/.55 \qquad (19)$$

Reefing line length, L_R, is the circumference of the canopy at the skirt. The total length of the reefing line would be L_R plus an additional length needed for splicing.

Forebody Interference Factor, K

The drag coefficient of a parachute deployed in the wake of a forebody is less than the free stream drag coefficient of the parachute. This reduction in drag coefficient is a function of the trailing distance of the parachute, the ratio of the parachute diameter to the forebody diameter, and the local flow conditions. The drag loss of hollow hemispheres in the presence of a forebody has been studied by Heinrich[10]. The data from Reference 10 reproduced as Figure 6 is used to determine the forebody interference factor. It is noted from Figure 6 that for a trailing distance of up to 5 nominal diameters a mean curve would be within ±2% error for a forebody size, D_P/D_B = 2 to 3. From this curve the interference factor K for L_s/D_o = 1.0 and λ_g = 0 is,

$$K = 0.854 + .044\left(\frac{x}{D_o}\right) - .004\left(\frac{x}{D_o}\right)^2, \qquad (20)$$

$$1 < x/D_o < 5$$

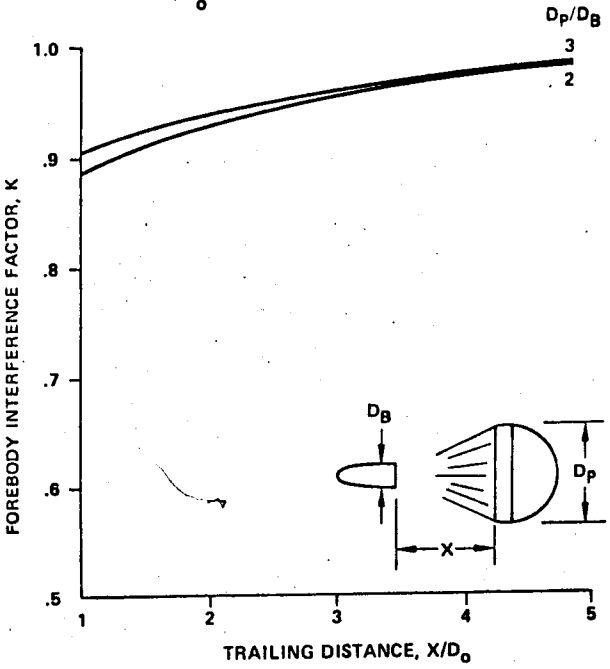

Fig. 6. Parachute drag loss as a function of trailing distance and forebody diameter. (Ref. 10)

The interference factor K is also a function of the suspension line length and the geometric porosity, that is,

$$K = f\left(\frac{L_s}{D_o}, \lambda_g\right) \qquad (21)$$

Figure 7 shows variation of the interference factor with suspension line length at a constant trailing distance. The curves have been extrapolated to $\frac{L_s}{D_o} = 1$, and K is replotted for $\frac{L_s}{D_o} = 1$ as a function of geometric porosity in Figure 8. This curve gives the variation of K with λ_g. Combining K from Figures 6, 7, and 8 we get,

$$K = 0.854 + .044\left(\frac{x}{D_o}\right) - .004\left(\frac{x}{D_o}\right)^2 + .1\left(\frac{L_s}{D_o} - 1\right) + .422\,\lambda_g - 3.7\,(\lambda_g)^2 \qquad (22)$$

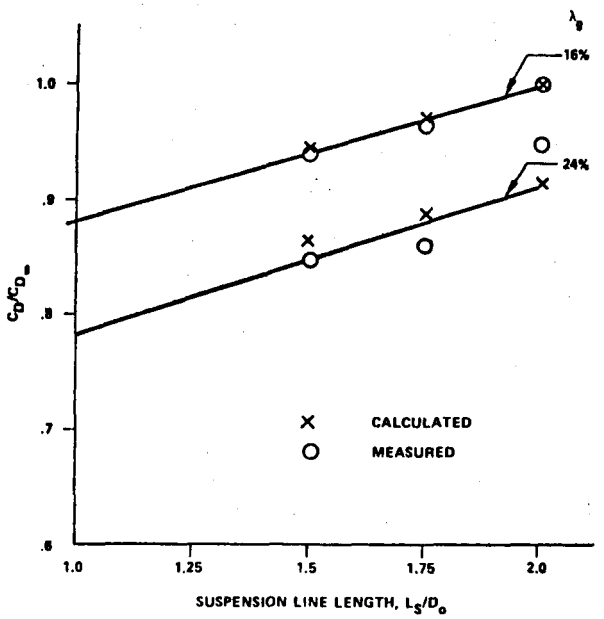

Fig. 7. Effect of suspension line length on forebody interference factor.

The interference factor K is estimated for a special case in which the forebody centerline is in line with the longitudinal axis of the parachute. It may not be applicable for angles of attack.

Modified K_R In The Presence of Forebody - K'_R

Wind tunnel results show that the correction factor K_R which is otherwise independent of the suspension line length, l_s, and the geometric porosity, λ_g, becomes dependent on these two parameters in the presence of a forebody. Thus K_R should be modified to include wake effects. Figures 9 and 10 are plots of K_R, showing the

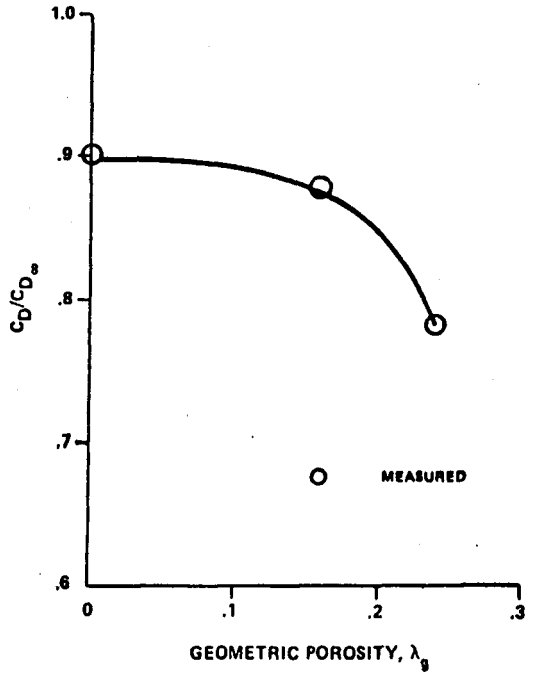

Fig. 8. Effect of geometric porosity on forebody interference factor

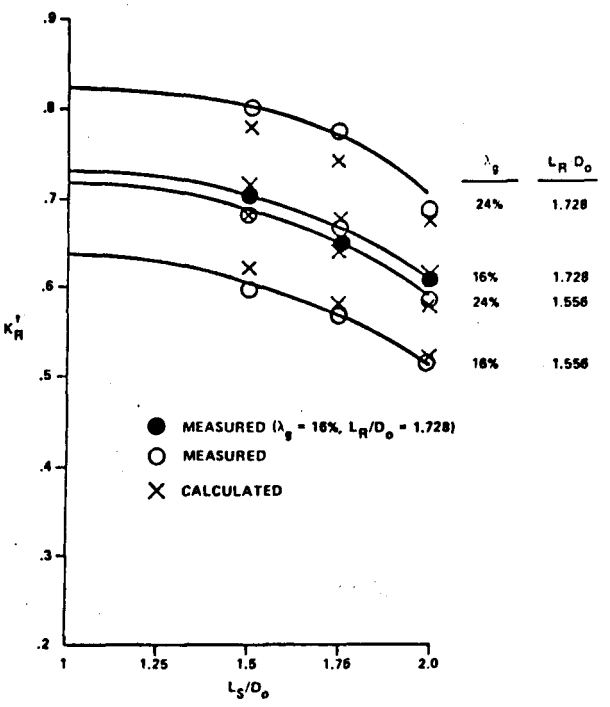

Fig. 9. Effect of suspension line length on K_R in forebody wake.

variation with L_s/D_o and λ_g respectively, in the presence of a forebody. The curves were extrapolated to the basic suspension line length ratio of one to determine the variation of K'_R with L_s/D_o. Since the curves for different geometric porosities were essentially parallel, the

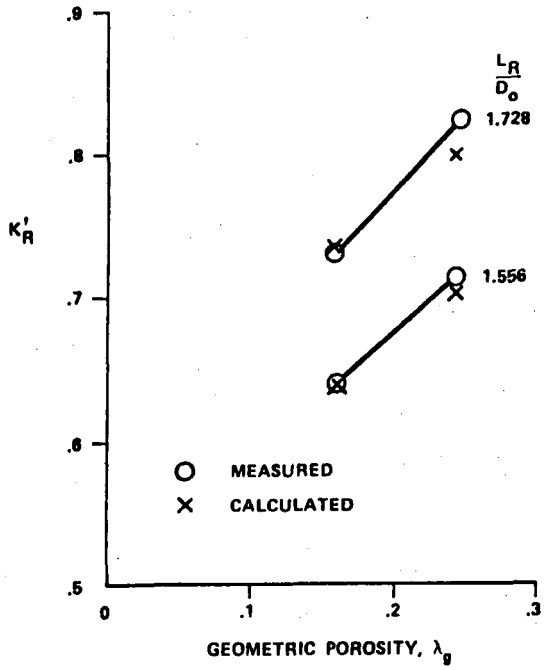

Fig. 10. Effect of geometric porosity on K_R in forebody wake.

variation with geometric porosity was determined using the extrapolated results for $L_s/D_o = 1.0$. These two plots have been combined to yield a modified drag area ratio for the reefed chute.

$$K'_R = K_R + 0.36\left(\frac{L_s}{D_o}\right) - 0.16\left(\frac{L_s}{D_o}\right)^2 + 0.75\,\lambda_g - 0.425 \qquad (23)$$

It should be noted that the above expression for K'_R is valid only in the presence of a forebody. For a reefed canopy in free stream, $K'_R = K_R$, and for a full open canopy in the forebody wake $K'_R = 1$.

IV. Drag Coefficient of 20-Degree Conical Ribbon Parachute

Free Stream Conditions

Combining expressions for C_{D_1}, K_{λ_g} and K_{L_s/D_o}, the estimated drag coefficient of a full open 20-degree conical ribbon chute becomes,

$$C_{D_\infty} = 0.874 - 2.29\,\lambda_g + 1.953\,(\lambda_g)^2 + (0.055 + 1.145\,\lambda_g)\left(\frac{L_s}{D_o} - 1\right) + (0.012 - 0.775\,\lambda_g)\left(\frac{L_s}{D_o} - 1\right)^2 \qquad (24)$$

Reefed canopy drag coefficient estimates are obtained by multiplying equation (24) by the reefed factor K_R. The drag area ratio, K_R, is expressed as a function of reefing ratio as,

$$K_R = 1.735\left(\frac{D_R}{D_o}\right) - .11$$

or

$$K_R = 0.55\left(\frac{L_R}{D_o}\right) - .11 \quad . \qquad (25)$$

Forebody Interference Effects

The drag coefficient of a 20-degree conical ribbon parachute behind a forebody is given by equation (24) multiplied by a factor K, that is,

$$C_D = [0.874 - 2.29\,\lambda_g + 1.953(\lambda_g)^2 + (0.055 + 1.145\,\lambda_g)\left(\frac{L_s}{D_o} - 1\right) + (0.012 - 0.775\,\lambda_g)\left(\frac{L_s}{D_o} - 1\right)^2]\,K \qquad (26)$$

where

$$K = 0.854 + .044\left(\frac{x}{D_o}\right) - .004\left(\frac{x}{D_o}\right)^2 \quad . \qquad (27)$$

The drag coefficient of a reefed canopy behind a forebody is given by equation (26) multiplied by the drag area ratio K'_R.

where

$$K'_R = K_R + 0.36\left(\frac{L_s}{D_o}\right) - 0.16\left(\frac{L_s}{D_o}\right)^2 + 0.75\,\lambda_g - 0.425 \qquad (28)$$

V. Scaling Effects

The change in parachute drag coefficient due solely to a change in parachute size is the scaling effect. It is difficult to assess this change because there are many variables which change with size, and exact geometric scaling is not always possible. For example, in some cases it is not practical to construct a small model with the same number of gores as in the full scale, or with even the same number of horizontals and verticals. Also, the material selected for model fabrication may not permit the same flexibility as in full scale. A study[11] was conducted to develop some mathematical relationships to give scaling effects. However, experimental data used in the study came from various test programs using parachutes with different design parameters. This prevented determination of the change in parachute performance due to change in size alone.

Figure 11 presents a plot of the variation of drag coefficient for a 20-degree conical ribbon parachute with parachute size (its nominal diameter). The data for various size parachutes considered in this report has been converted to a case of $L_s/D_o = 1.0$ and two geometric porosities of 16 and 24 percent using the mathematical model

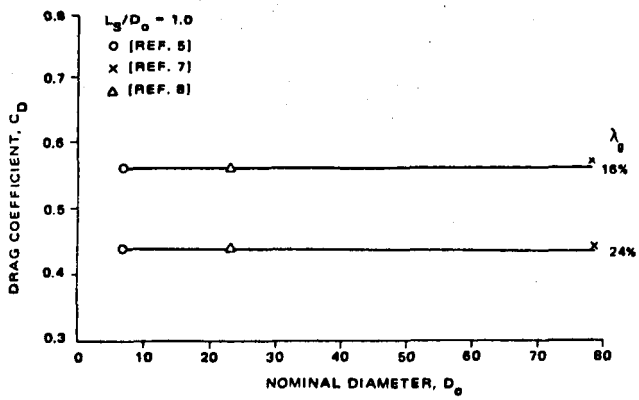

Fig. 11. Parachute scaling effect.

developed in this report. It is evident from the figure that the drag coefficient is essentially constant over the range of parachute sizes plotted. It is appropriate to mention that for small model parachutes[6,9] the empirical formula does not yield accurate results. This may be due in part to model flexibility and geometric non-similarity in model fabrication. The effect of these parameters has not been ascertained at the present time.

VI. Discussion

Equations (24) and (26) express the drag coefficient of a 20-degree conical ribbon parachute in free stream and in the forebody wake respectively. Figure 12 presents the computer program used to predict the drag coefficient of a 20-degree conical ribbon parachute for a given set of design parameters. Using this computer program, the drag coefficients of several parachute designs in free stream and in the forebody wake are tabulated in Tabels 2 and 3 respectively. These values are plotted against the experimental values in Figures 4, 7, 9, and 10.

The developed math model can predict the drag coefficient of a 20-degree conical ribbon parachute with a given suspension line length and geometric porosity within one percent of the available experimental and drop test data (see Figure 4).

The calculated reefed and full open drag coefficients of a 20-degree conical ribbon parachute behind a forebody agree within 6-percent of the available data (see Figures 7, 9, and 10).

The derived mathematical expression can predict the drag coefficient of a 20-degree conical ribbon parachute for a wide range of the parachute size (6.75 ft D_o to 78.3 ft D_o). However, the empirical formulation does not predict the drag coefficients for chute sizes less than 6.75 ft D_o accurately. This may be due in part to model flexibility and geometric nonsimilarity in model fabrication.

```
// *  LAJPAT,9230,  X243

// FOR
*IOCS(1132PRINTER,CARD)
*ONE WORD INTEGERS
*LIST SOURCE PROGRAM
      DIMENSION IA(40),IB(40)
      IN=2
      IO=3
      XKT=1.0
  17  WRITE(IO,18)
  18  FORMAT(1H1)
   1  WRITE(IO,2)
   2  FORMAT(///)
      READ(IN,3) IA,IB
   3  FORMAT(40A2)
      WRITE(IO,6) IA,IB
   6  FORMAT(5X,40A2,//,40A2,/)
   4  READ(IN,5)XLG,XLS,XLR,XLT,XDB,IFLG,IFB,IFR
   5  FORMAT(5F8.0,3I5)
      XTEM=XLS-1.0
      IF(IFR)16,30,16
  16  XKR=1.0
      GO TO 19
  30  XKR=0.55*XLR-0.11
  19  IF(IFB)26,20,26
  20  XK=1.0
  26  IF(IFR)23,22,23
  22  IF(IFB)50,23,50
  50  XKR=XKR+0.36*XLS-(0.16*XLS*XLS)+0.75*XLG-0.425
  23  IF(IFB)24,27,24
  24  XK=0.854+0.044*XLT-0.004*(XLT*XLT)+0.1*XTEM+(0.422-3.7*XLG)*XLG
  27  CD=(0.874+(-2.290+1.953*XLG)*XLG+(0.055+1.1450*XLG)*XTEM-(-.012
     *+0.775*XLG)*(XTEM*XTEM))*XKR*XK
      IF(IFR)32,34,32
  32  WRITE(IO,10)XLS,XLT,XLG,XLR,XK,CD
      GO TO 11
  34  WRITE(IO,10)XLS,XLT,XLG,XLR,XKR,CD
  10  FORMAT(5X,5F10.3,F10.4)
  11  IF(IFLG)1,4,25
  25  IF(IFLG-1)17,17,12
  12  CALL EXIT
      END
```

Fig. 12. Computer Program of the Math Model

Table 2. Free Stream Drag Coefficients

FULL OPEN , FREE STREAM DRAG COEFFICIENTS

LS/D0	X/D0	LG	LR/D0	K	CD
1.000	2.000	0.160	2.011	1.000	0.5575
1.500	2.000	0.160	2.011	1.000	0.6486
1.750	2.000	0.160	2.011	1.000	0.6732
2.000	2.000	0.160	2.011	1.000	0.6837
1.000	2.000	0.240	2.011	1.000	0.4368
1.500	2.000	0.240	2.011	1.000	0.5582
1.750	2.000	0.240	2.011	1.000	0.5863
2.000	2.000	0.240	2.011	1.000	0.5926

REEFED FREE STREAM DRAG COEFFICIENTS

LS/D0	X/D0	LG	LR/D0	KR	CD
1.000	2.000	0.160	1.728	0.840	0.4686
1.500	2.000	0.160	1.728	0.840	0.5451
1.750	2.000	0.160	1.728	0.840	0.5657
2.000	2.000	0.160	1.728	0.840	0.5746
1.000	2.000	0.240	1.728	0.840	0.3671
1.500	2.000	0.240	1.728	0.840	0.4691
1.750	2.000	0.240	1.728	0.840	0.4927
2.000	2.000	0.240	1.728	0.840	0.4980

REEFED FREE STREAM DRAG COEFFICIENTS

LS/D0	X/D0	LG	LR/D0	KR	CD
1.000	2.000	0.160	1.556	0.745	0.4158
1.500	2.000	0.160	1.556	0.745	0.4837
1.750	2.000	0.160	1.556	0.745	0.5021
2.000	2.000	0.160	1.556	0.745	0.5099
1.000	2.000	0.240	1.556	0.745	0.3258
1.500	2.000	0.240	1.556	0.745	0.4163
1.750	2.000	0.240	1.556	0.745	0.4373
2.000	2.000	0.240	1.556	0.745	0.4420

Table 3. Drag Coefficients in Forebody Wake

FULL OPEN DRAG COEFFICIENTS IN A FOREBODY WAKE

LS/DO	X/DO	LG	LR/DO	K	CD
1.000	2.000	0.160	2.011	0.898	0.5011
1.500	2.000	0.160	2.011	0.948	0.6154
1.750	2.000	0.160	2.011	0.973	0.6556
2.000	2.000	0.160	2.011	0.998	0.6829
1.000	2.000	0.240	2.011	0.814	0.3557
1.500	2.000	0.240	2.011	0.864	0.4824
1.750	2.000	0.240	2.011	0.889	0.5213
2.000	2.000	0.240	2.011	0.914	0.5418

REEFED DRAG COEFFICIENTS IN A FOREBODY WAKE

LS/DO	X/DO	LG	LR/DO	KR	CD
1.000	2.000	0.160	1.728	0.735	0.3685
1.500	2.000	0.160	1.728	0.715	0.4403
1.750	2.000	0.160	1.728	0.675	0.4427
2.000	2.000	0.160	1.728	0.615	0.4203
1.000	2.000	0.240	1.728	0.795	0.2829
1.500	2.000	0.240	1.728	0.775	0.3740
1.750	2.000	0.240	1.728	0.735	0.3834
2.000	2.000	0.240	1.728	0.675	0.3659

REEFED DRAG COEFFICIENTS IN A FOREBODY WAKE

LS/DO	X/DO	LG	LR/DO	KR	CD
1.000	2.000	0.160	1.556	0.640	0.3211
1.500	2.000	0.160	1.556	0.620	0.3820
1.750	2.000	0.160	1.556	0.580	0.3807
2.000	2.000	0.160	1.556	0.520	0.3556
1.000	2.000	0.240	1.556	0.700	0.2492
1.500	2.000	0.240	1.556	0.680	0.3284
1.750	2.000	0.240	1.556	0.640	0.3340
2.000	2.000	0.240	1.556	0.580	0.3146

VII. References

1. Anonymous, "Performance of and Design Criteria for Deployable Aerodynamic Decelerators", ASD-TR-61-579, December 1963, Air Force Flight Dynamics Laboratory, Wright-Patterson Air Force Base, Ohio.

2. Bacchus, D. L., et al., "Wind Tunnel Investigation of Space Shuttle Solid Rocket Booster Drogue Parachutes and Deployment Concepts", AIAA Paper 75-1366, AIAA 5th Aerodynamic Deceleration Systems Conference, Albuquerque, New Mexico, November 17-19, 1975.

3. Utreja, L. R., "Wind Tunnel Dynamic Pressure to Duplicate Full Scale Steady State Drag Coefficient of the SRB Drogue Chute", Northrop Services, Inc., Informal Memorandum M-9230-75-378, March 1975.

4. Knacke, T., and Hegele, A., Model Parachutes, Comparison Tests of Various Types, Memorandum Report MCREXE-672-12B, 12 January 1949.

5. Utreja, L. R., "Wind Tunnel Test of the Space Shuttle Solid Rocket Booster Drogue Parachute System", Northrop Services, Inc., TR-230-1342, September 1974.

6. Riffle, A. B., "Determination of the Aerodynamic Drag and Static Stability of Reefed Parachute Canopies", AFFDL-TR-64-166, January 1965.

7. Holt, I. T., "Design and Development of a Heavy Duty 76-ft Ribbon Parachute", Proceedings Aerodynamic Deceleration Systems Conference, Technical Report No. 69-11, April 1969.

8. Maydew, R. C., and Johnson, D. W., "Supersonic and Transonic Deployment of Ribbon Parachutes at Low Altitude", Royal Aeronautical Society Symposium on Parachutes and Related Technologies, September 1971.

9. Holbrook, J. W., "Sandia Corporation Pressure and Disreefing Test of Model Parachutes in the Vought System Divisions Low Speed Wind Tunnel", LSWT-445, September 1974.

10. Heinrich, H. G. and Haak, E. L., "The Drag of Cones, Plates, and Hemispheres in the Wake of a Forebody in Subsonic Flow", ASD-TR61-587, December 1961.

11. Walcott, W. B., "Study of Parachute Scale Effects", ASD-TDR-62-1023, January 1963.